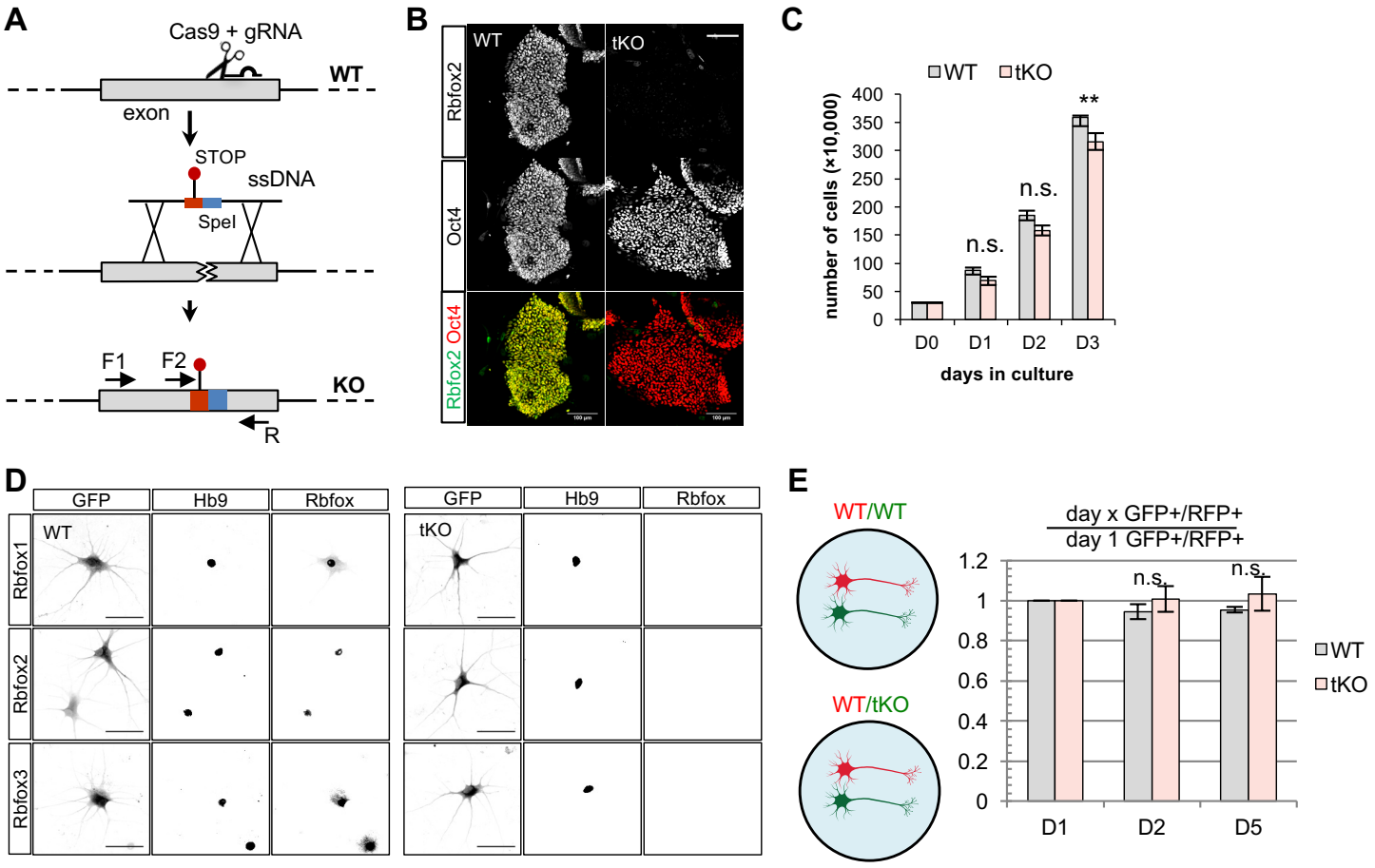

Figure S1. Generation and characterization of *Rbfox1-3* triple knockout (*Rbfox* tKO) mESC lines and mESC-derived motor neurons. Related to **Figure 2**. (A) Schematic illustration of CRISPR/Cas9-mediated genome engineering to generate knockout mES cell line in which all *Rbfox* genes are disrupted by insertion of two in-frame stop codons that are part of an 11-nt insertion additionally disrupting the downstream reading frame. PCR primers used for genotyping are indicated by black arrows. (B) *Rbfox* tKO does not affect expression of stem cell pluripotency marker Oct4. Scale bar: 100 μm. (C) *Rbfox* tKO mES cells show similar rate of proliferation compared to wild-type controls (two-way repeated measures ANOVA, post hoc Bonferroni's multiple comparisons test, **p<0.01, n.s. p>0.05, n=3; error bars represent standard error of the mean (S.E.M.). (D) Validation of Rbfox1-3 protein depletion in *Rbfox* tKO motor neurons based on immunostaining analysis on day 5. Neuronal morphology was visualized by expression of GFP from transfected plasmid and motor neurons were identified by antibody staining of the endogenous Hb9 protein. Depletion of Rbfox proteins is determined by antibody that specifically recognizes each family member. (E) Quantitative analysis of survival of wild-type and *Rbfox* tKO motor neurons in long-term culture. Schematic illustration of a two-color assay is shown on the left. Normalized survival is shown on the right (two-way repeated measures ANOVA, post hoc Bonferroni's multiple comparisons test, n.s. p>0.05, average N=60 in each group, n=3 biological replicates; error bars represent S.E.M..

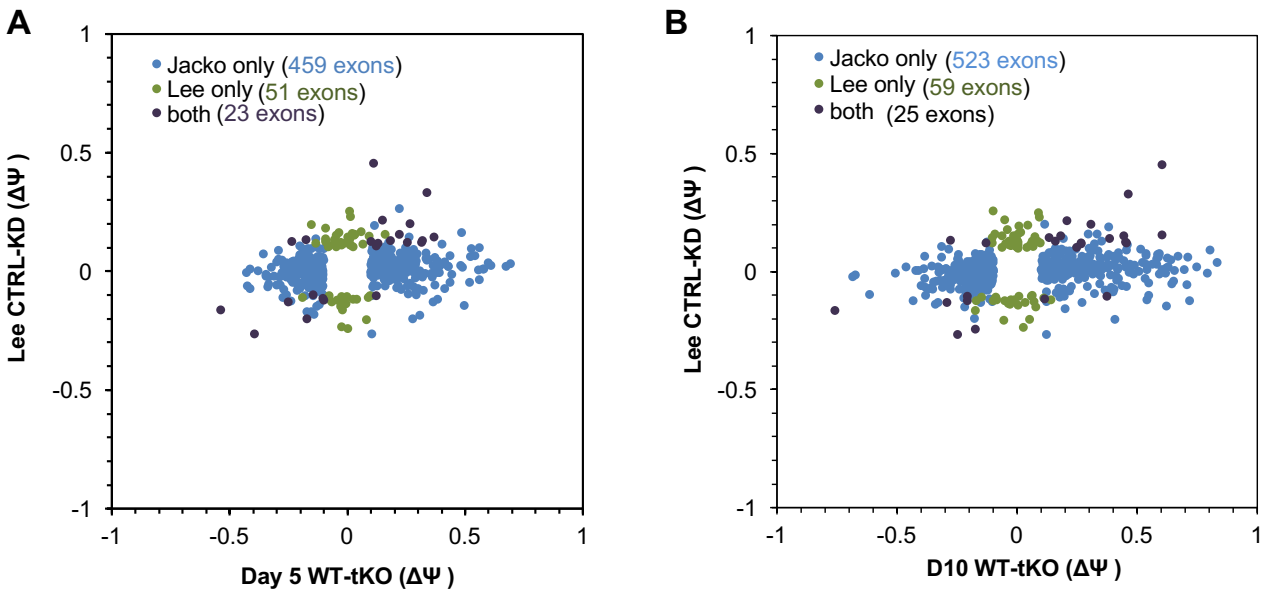

Figure S2. Comparison of splicing changes in *Rbfox* tKO neurons (Jacko et al., this study) and in *Rbfox1* and *3* double knockdown hippocampal neurons (Lee et al). Related to **Figure 2**. Only cassette exons with sufficient read depth (≥20 reads) in both datasets and with splicing changes in at least one dataset (|ΔΨ|≥0.1 and FDR≤0.05) are shown. (A) day 5 neurons. (B) day 10 neurons.

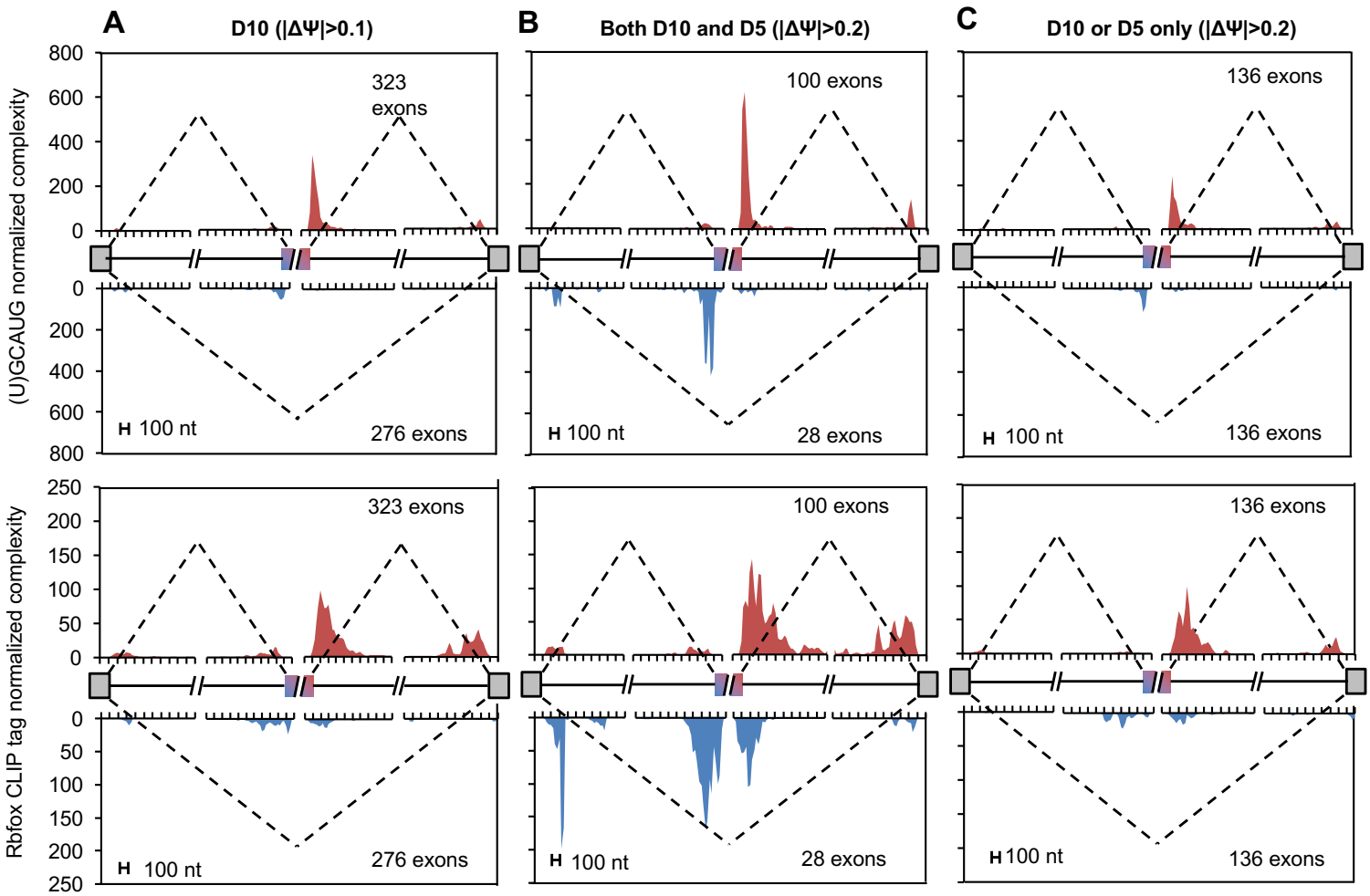

Figure S3. RNA-maps that predict Rbfox-dependent splicing from the position of the binding sites. Related to **Figure 2**. In each panel, normalized (U)GCAUG (top) or CLIP (bottom) score in the alternative exon or flanking intronic sequences is shown. Exons with Rbfox-dependent inclusion are shown in red and exons with Rbfox-dependent exclusion are shown in blue. (A) Rbfox-dependent exons on day 10 ($|\Delta\Psi| \geq 0.1$ and FDR$\leq$0.05). (B) Rbfox-dependent exons on both day 5 and day 10 ($|\Delta\Psi| \geq 0.2$ and FDR$\leq$0.05). (C) Rbfox-dependent exons on either day 5 or day 10, but not both ($|\Delta\Psi| \geq 0.1$ and FDR$\leq$0.05).

A

Rbfox targets excluded

	overall		Rbfox targets		Nova targets		Mbnl targets		Ptbp targets	
	WT	tKO	WT	tKO	WT	tKO	WT	tKO	WT	tKO
D5	2	2	2	1	2	3	3	3	2	2
D10	4	2	4	1	4	4	4	4	4	4

maturation stage change: +1 0 -1 -2 -3

B

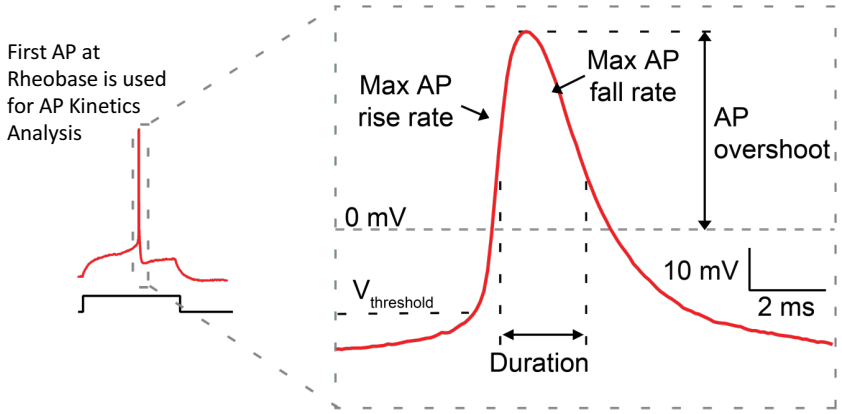

C

	WT ± SEM	*Rbfox* tKO ± SEM	Significance (red: p < 0.05)
Input Resistance (MOhm)	232 ± 27 *n* = 31	352 ± 34 *n* = 27	*p* = 0.0071
Rheobase (pA)	97 ± 12 *n* = 31	54 ± 7.6 *n* = 27	*p* = 0.0068
Capacitance (pF)	131 ± 6.5 *n* = 30	104 ± 9.2 *n* = 27	*p* = 0.0171
Resting Membrane Potential (mV)	-57 ± 0.78 *n* = 31	-56 ± 0.95 *n* = 26	*p* = 0.209
Action Potential Duration (ms)	1.8 ± 0.07 *n* = 31	1.9 ± 0.17 *n* = 27	*p* = 0.415
Action Potential Overshoot (mV)	36 ± 1.3 *n* = 31	38 ± 1.4 *n* = 27	*p* = 0.396
Action Potential Max Rise Rate (mV/ms)	94 ± 4.0 *n* = 31	93 ± 5.6 *n* = 27	*p* = 0.801
Action Potential Max Fall Rate (mV/ms)	-40 ± 2.2 *n* = 31	-40 ± 3.1 *n* = 27	*p* = 0.963
Action Potential Threshold (mV)	-35 ± 0.7 *n* = 31	-32 ± 0.6 *n* = 27	*p* = 0.0125
Max Number of Action Potentials	31.5 ± 1.4 *n* = 31	24.0 ± 2.1 *n* = 27	*p* = 0.0029

D

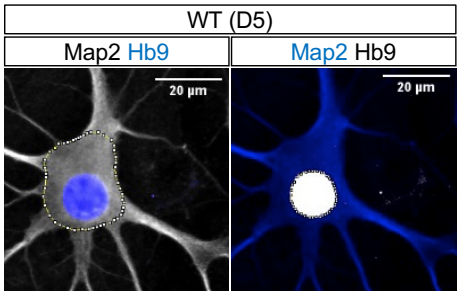

E

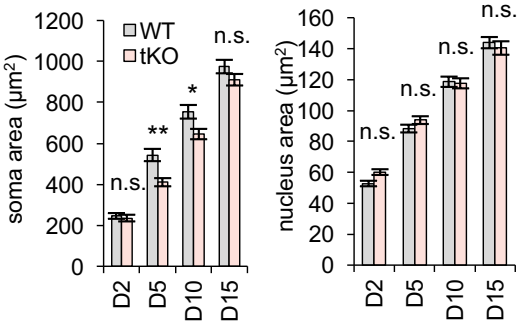

Figure S4. Immature splicing, electrophysiological and morphological features of *Rbfox* tKO motor neurons. Related to **Figure 3**. (A) Specific perturbation of Rbfox target exons results in global changes in the developmental splicing program. Exons coregulated by Rbfox were excluded from target exons regulated by Nova, Mbnl or Ptbp. (B) Illustration showing representative analysis of action potential kinetics. (C) Summary of quantitative analysis of electrophysiological recordings of WT and Rbfox tKO motor neurons on day 5. Unpaired Student's t-test was used for statistical comparison. (D) Illustration of cell body size (left) and nuclear size (right) measurement. Scale bar: 20 μm. (E) Quantitative analysis of cell body size (left) and nuclear size (right) in day 5 WT and tKO motor neurons during maturation (two-way repeated measures ANOVA, post hoc Bonferroni's multiple comparisons test, ** $p<0.01$, * $p<0.05$, N=60-80 in each group, n=4 biological replicates, error bars represent S.E.M.).

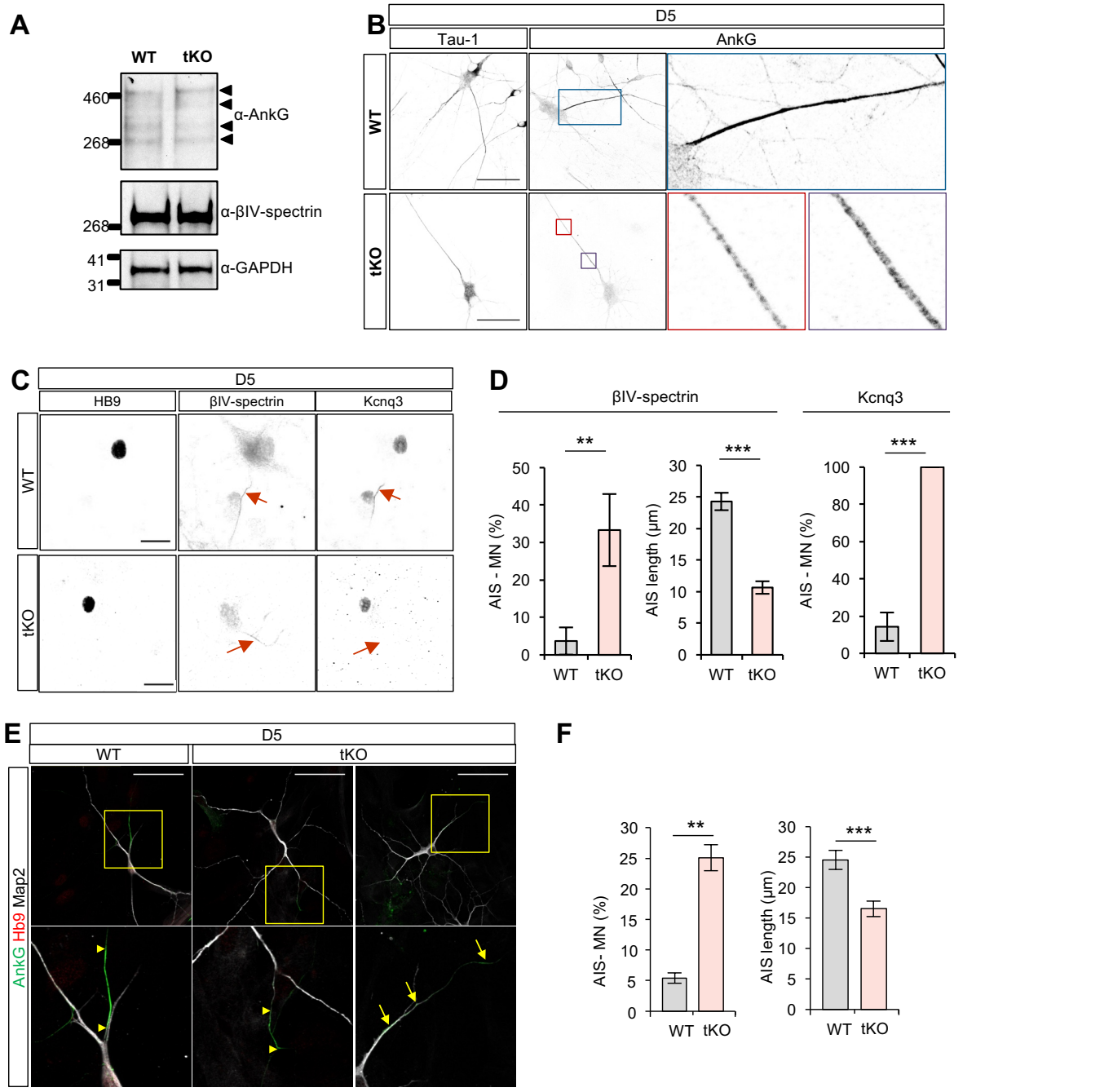

Figure S5. Characterization of AIS defects in Rbfox tKO motor neurons and ventral interneuron. Related to **Figure 5.** (A) Comparison of AnkG and βIV-spectrin protein levels in day 5 WT and Rbfox tKO motor neurons using immunoblot analysis. Multiple bands representing AnkG splicing variants are indicated. GAPDH is shown as a loading control. (B) Immunostaining of AnkG and Tau-1 shows AnkG puncta at weaker intensity in the distal region of the axon in day 5 Rbfox tKO motor neurons. Fluorecence intensity in the zoom-in views is enhanced to highlight the distributed AnkG puncta. Scale bar: 50 μm. (C) Immunostaining of βIV-spectrin and Kcnq3 in day 5 WT and tKO motor neurons on day 5. Scale bar: 20 μm. (D) Quantification of WT and *Rbfox* tKO motor neurons that lack βIV-spectrin or Kcnq3 accumulation in the proximal axon or have reduced AIS length based on staining intensity. Fisher's exact test was used to compare the proportion of AIS- neurons, and the error bars represent S.E.M. estimated from Binomial distribution. AIS length was compared using t-test, and error bars represent S.E.M. AIS length was not compared for Kncq3 staining due to lack of Kncq3 positive cells on day 5. (***p<0.001, **p<0.01; N=51 for βIV-spectrin staining and N=38 for Kncq5 staining; samples are pooled from 3 biological replicates). (E) Immunostaining of an AIS marker AnkG in day 5 WT and *Rbfox* tKO ventral spinal interneurons (Map2+, Hb9-). Scale bar: 50 μm. Arrow heads indicate boundaries of AIS staining. Arrows indicate punctate AIS staining observed in some tKO interneurons. (F) AIS quantification in WT and *Rbfox* tKO interneurons (t-test, ***p<0.001, **p<0.01; N ranges from 51-60 for each group, n=3 biological replicates).

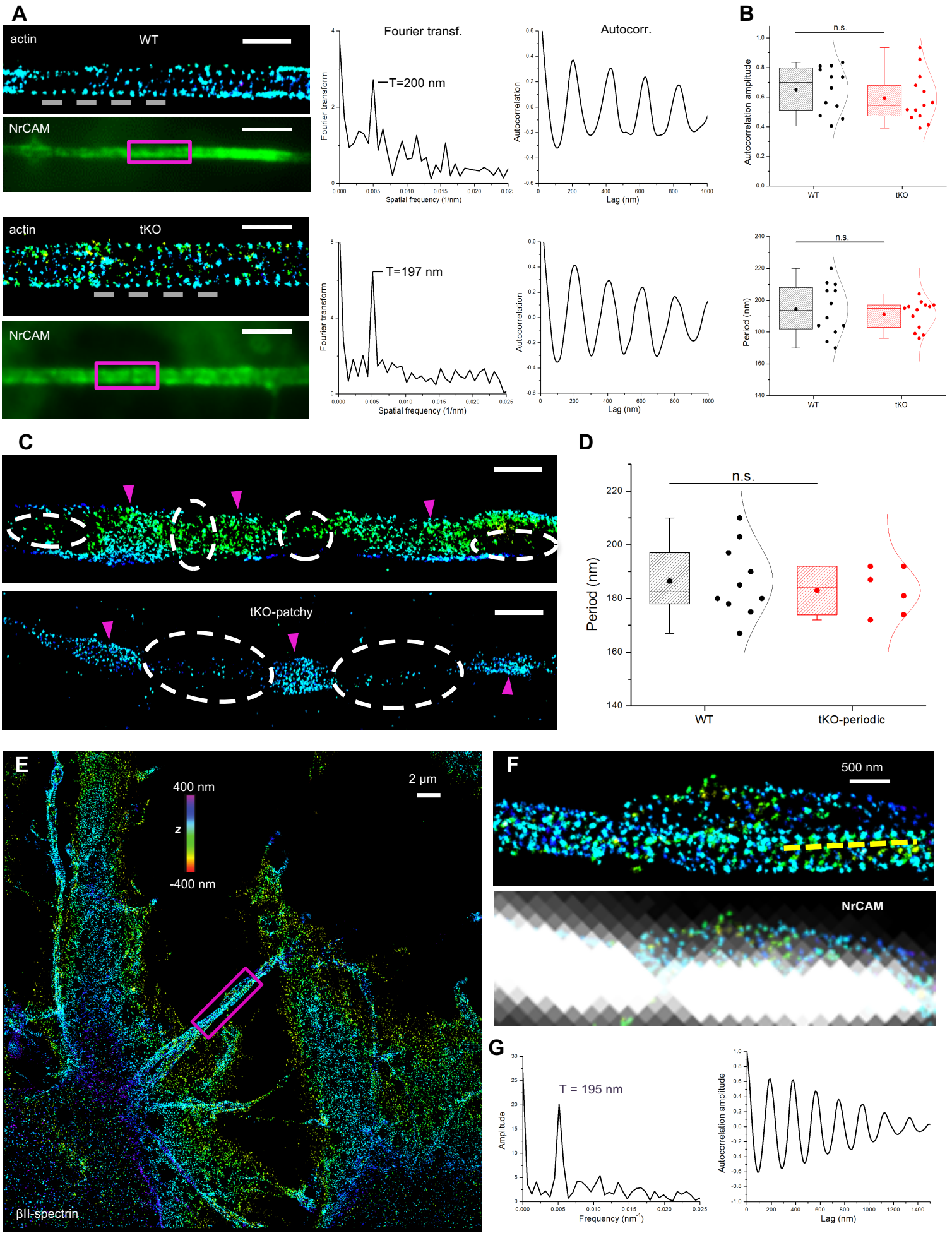
A
actin
WT
NrCAM
Fourier transf.
T=200 nm
Fourier transform
Spatial frequency (1/nm)
Autocorr.
Autocorrelation
Lag (nm)
actin
tKO
NrCAM
T=197 nm
B
n.s.
Autocorrelation amplitude
WT
tKO
n.s.
Period (nm)
WT
tKO
C
tKO-patchy
D
n.s.
Period (nm)
WT
tKO-periodic
E
400 nm
z
-400 nm
2 µm
βII-spectrin
F
500 nm
NrCAM
G
T = 195 nm
Amplitude
Frequency (nm-1)
Autocorrelation amplitude
Lag (nm)

Figure S6. 3D-STORM imaging of AIS in day 10 WT and *Rbfox* tKO AIS motor neurons. Related to **Figure 5.** (A) Representative 3D-STORM images and quantitative analyses of actin in WT and tKO AIS. Left: 3D-STORM of actin stained with phalloidin-AF647 (top) and epifluorescence image of immunolabeled NrCAM (bottom) as a marker for AIS. The STORM images correspond to the regions marked by magenta boxes. Scale bars, 1 μm for the top images and 5 μm for the bottom. Middle and right: Fourier transform (middle) and autocorrelation analyses (right) of actin axial distribution in the indicated regions of AIS in the left panel (grey dashed lines). (B) Box plots of average autocorrelation amplitude (top) and repeating period (bottom) of actin in wild-type and tKO AIS. No significant difference is shown by two-tailed Student's t-test (p=0.39 and 0.54, respectively). Raw data were plotted to the right of the boxes with fitting curves of normal distribution. n=12 for wild-type and n=13 for tKO AIS from three independent experiments. (C) Additional examples of tKO AIS with patchy ankyrin G. White ovals and magenta arrowheads show alternating patterns of sparse and dense ankyrin G, respectively. Scale bars, 2 μm. (D) Spacing of ankyrin G in the small fraction of *Rbfox* tKO AIS with periodic ankyrin G is similar to the WT. Box plot of the average period of ankyrin G in wild-type and periodic tKO AIS. No significant difference is shown by two-tailed Student's t-test (p=0.58). Raw data were plotted to the right of the boxes with fitting curves of normal distribution. (E) A 3D-STORM image of WT neurons immunostained against βII-spectrin. (F) top: Zoom-in of the region in the magenta box in (E). bottom: Epifluorescence image of co-stained NrCAM, an AIS marker, overlaid with the 3D-STORM image. (G) Fourier transform (left) and autocorrelaton analysis (right) of the region marked by yellow dashed line in (F). A peak corresponding to 195 nm spacing was observed.

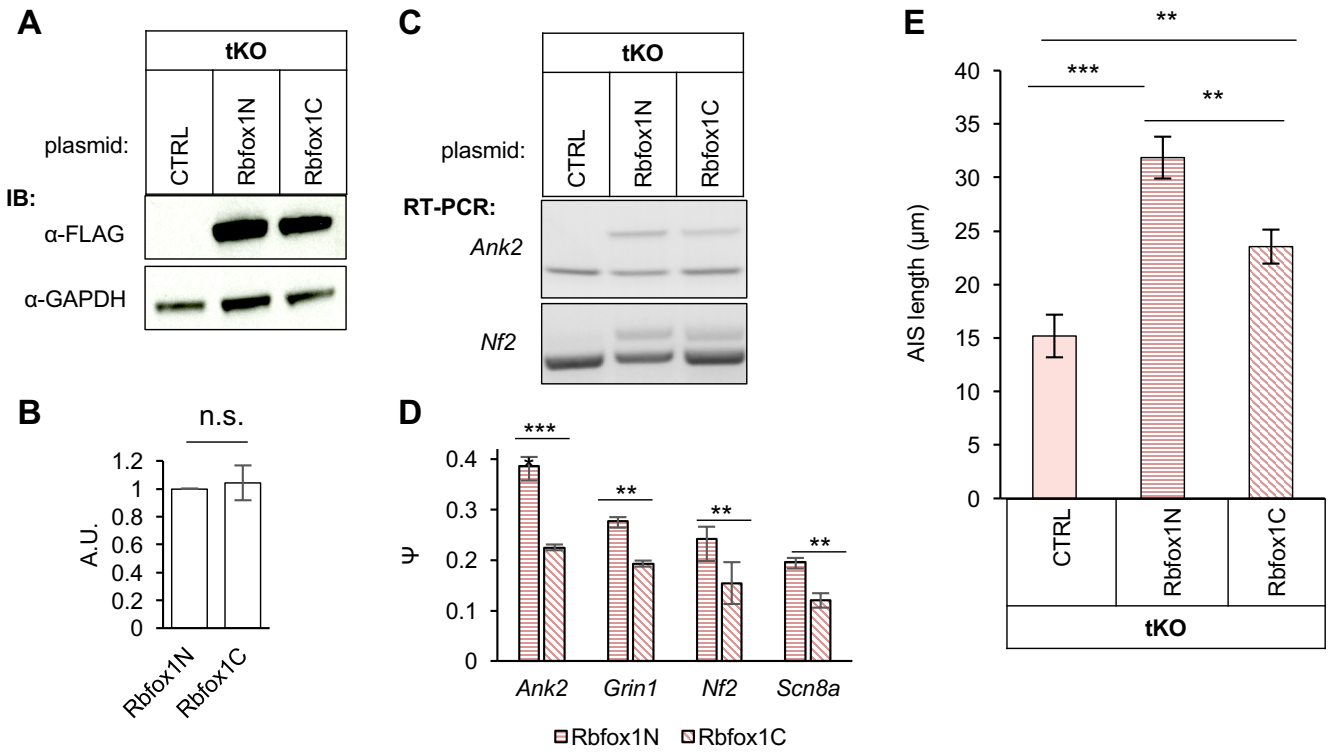

Figure S7: Rescue of alternative splicing and AIS defects in *Rbfox* tKO motor neurons by overexpression of Rbfox1 protein isoforms. Related to **Figure 6**. (A) Immunoblot analysis to validate the expression of FLAG-tagged Rbfox1 protein isoforms after plasmid transfection. GAPDH is used as a loading control. (B) Quantification of FLAG-Rbfox overexpression based on immunoblots (t-test, n=3 replicates). (C) RT-PCR of alternative splicing rescue for two representative Rbfox target exons. (D) Quantification of four representative Rbfox target exons (two-way ANOVA, post hoc Tukey's multiple comparisons test, ***p<0.001, **p<0.01, n=3 replicates, error bars represent S.E.M.). (E) Quantification of AIS length in *Rbfox* tKO neurons with or without expression of Rbfox1 protein isoforms (one-way ANOVA, post hoc Tukey's multiple comparisons test, ***p<0.001, **p<0.01, N ranges from 59 to 63 for each group, n=3 replicates). Error bars represent S.E.M..

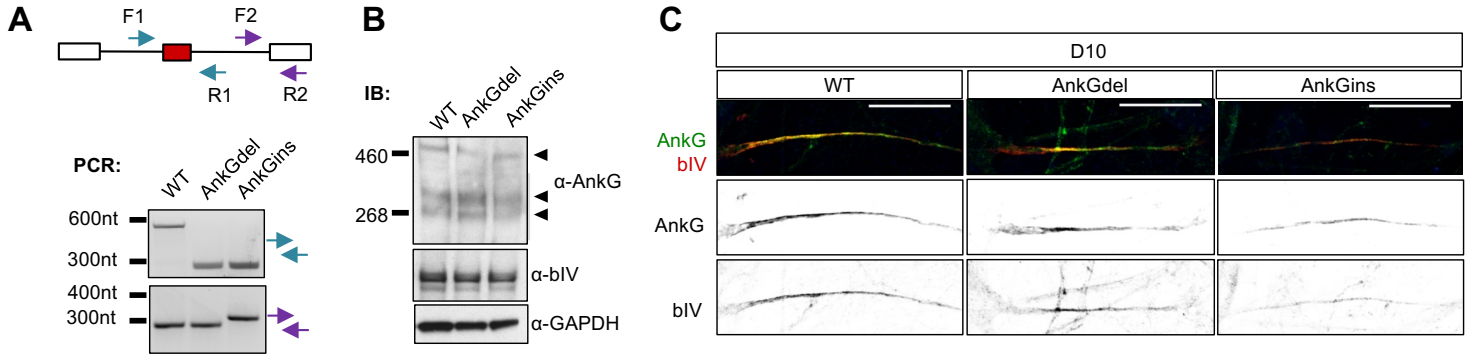

D

	WT ± SEM	AnkGins ± SEM	Significance (red: p < 0.05)
Input Resistance (MOhm)	573 ± 46 *n* = 28	602 ± 55 *n* = 26	*p* = 0.689
Rheobase (pA)	24 ± 2.5 *n* = 27	24 ± 2.6 *n* = 25	*p* = 0.937
Capacitance (pF)	177 ± 14 *n* = 27	177 ± 16 *n* = 26	*p* = 0.982
Resting Membrane Potential (mV)	-60 ± 1.2 *n* = 27	-59 ± 1.1 *n* = 26	*p* = 0.448
Action Potential Duration (ms)	2.8 ± 0.14 *n* = 27	3.4 ± 0.19 *n* = 25	*p* = 0.0081
Action Potential Overshoot (mV)	30 ± 1.7 *n* = 27	23 ± 1.3 *n* = 25	*p* = 0.0027
Action Potential Max Rise Rate (mV/ms)	62 ± 4.4 *n* = 27	41 ± 3.0 *n* = 25	*p* = 0.0005
Action Potential Max Fall Rate (mV/ms)	-25 ± 1.7 *n* = 27	-18 ± 1.5 *n* = 25	*p* = 0.0043
Action Potential Threshold (mV)	-32 ± 1.0 *n* = 27	-30 ± 0.70 *n* = 25	*p* = 0.180
Max Number of Action Potentials	13.4 ± 1.6 *n* = 27	9.0 ± 1.2 *n* = 25	*p* = 0.038

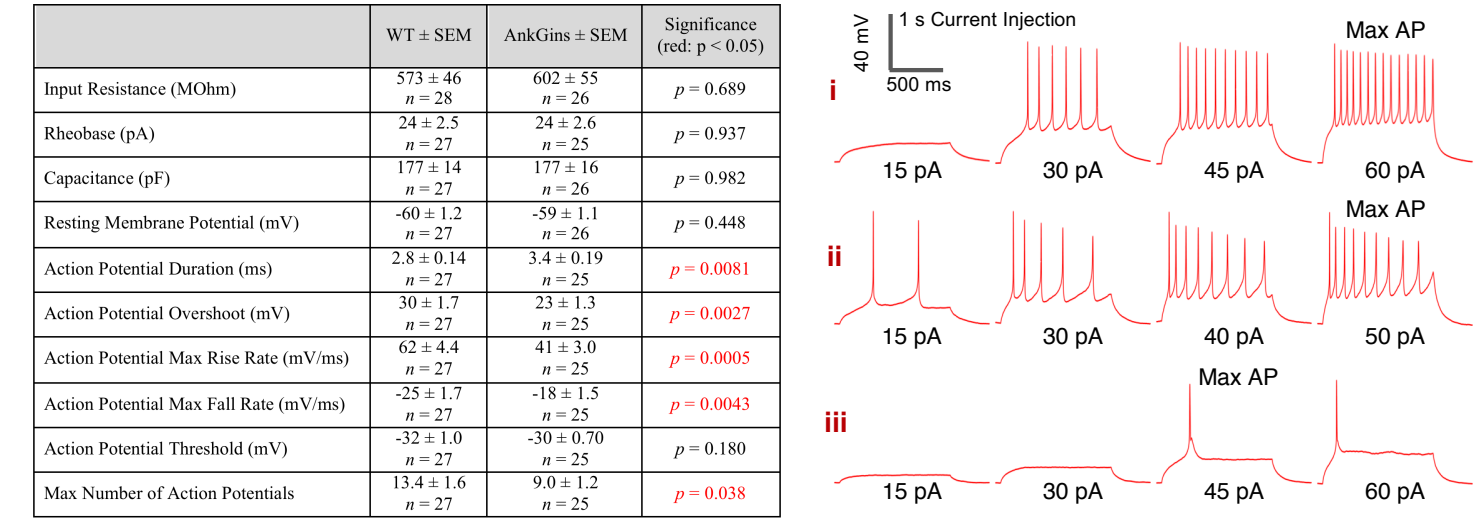

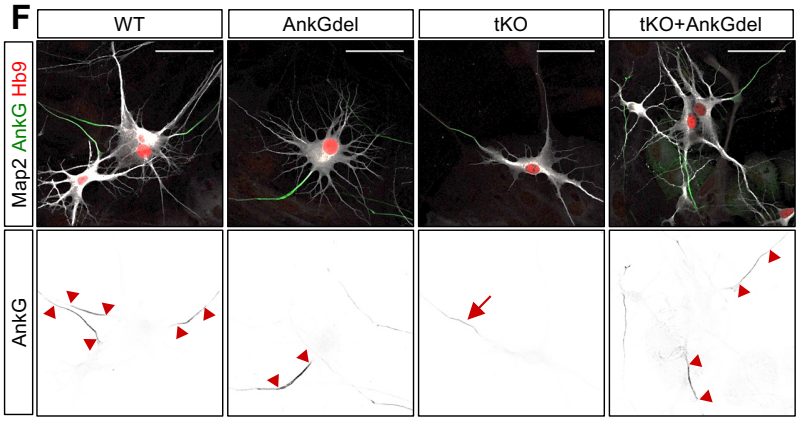

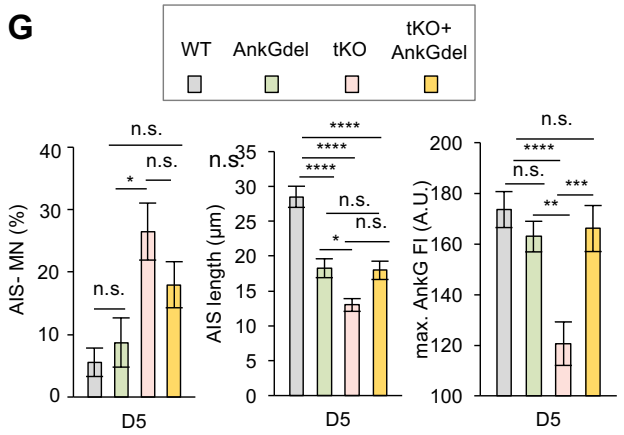

Figure S8. Disruption of the AIS in motor neurons by forced expression of AnkG splice variants. Related to **Figure 8**. (A) PCR genotyping of AnkGdel and AnkGins mutants generated by CRISPR/Cas9 genome engineering. (B) Immunoblot analysis of AnkG and βIV-spectrin protein levels in day 5 WT, AnkGdel and AnkGins motor neurons. Multiple bands representing AnkG protein variants are indicated. GAPDH is shown as a loading control. (C) βIV-spectrin localization to AIS is perturbed in AnkGins motor neurons. The AIS was co-immunostained with βIV-spectrin and AnkG antibody on day 10. Representative images of AIS in WT, AnkGdel and AnkGins motor neurons are shown. Scale bar: 20 μm. (D) Summary of quantitative analysis of electrophysiological recordings for WT and AnkGins neurons on day 5. (E) Recordings correspond with representative neurons displayed in Figure 8H. Representative 1s current steps for all electrophysiological recordings presented in this report. (F) Representative images of WT, tKO motor neurons, as well as motor neurons with AnkG exon deletion (AnkGdel) in WT or tKO background, on D5 of maturation. (G) Quantification of AIS negative motor neurons, AIS length, and maximum fluorescence intensity of AnkG immunostaining (one-way ANOVA, post hoc Tukey's multiple comparisons test, ****p<0.0001, ***p<0.001, **p<0.01, *p<0.05 n.s. p>0.05; N ranges from 62 to 66, n = 3 biological replicates). Error bars represent S.E.M.